Journal of Applied Polymer Science

Effect of Polymer Matrix/Montmorillonite Compatibility on Morphology and Melt Rheology of Polypropylene Nanocomposites

Shipeng Zhu,[1,2] Jinyao Chen,[1,2] Huilin Li,[1,2] Ya Cao[1,2]

[1]State Key Laboratory of Polymer Materials Engineering, Chengdu 610065, People's Republic of China
[2]Polymer Research Institute of Sichuan University, Chengdu 610065, People's Republic of China
Correspondence to: H. Li (E-mail: nic7703@scu.edu.cn) or Y. Cao (E-mail: caoya@scu.edu.cn)

ABSTRACT: In this study, Ca^{2+}-montmorillonite (Ca^{2+}-MMT) and organo-montmorillonite (OMMT) were modified by three compatibilizers with different degrees of polarity [poly(ethylene glycol) (PEG), alkyl-PEG, and polypropylene (PP)-*g*-PEG]. PP/MMT nanocomposites were prepared by melt blending and characterized using X-ray diffraction and transmission electron microscopy. The results showed the degree of dispersion of OMMT in the PP/PP-*g*-PEG/OMMT (PMOM) nanocomposite was considerably higher than those in the PP/PEG/OMMT and PP/alkyl-PEG/OMMT nanocomposites, which indicated that the dispersion was relative to the compatibility between modified OMMT and PP matrix. Linear viscoelasticity of PP/MMT nanocomposites in melt states was investigated by small amplitude dynamic rheology measurements. With the addition of the modified MMT, the shear viscosities and storage modulus of all the PP/MMT nanocomposites decreased. It can be attributed to the plasticization effect of PEG segments in the three modifiers. This rheological behavior was different from most surfactant modified MMT nanocomposites which typically showed an increase in dynamic modulus and viscosity relative to the polymer matrix. The unusual rheological observations were explained in terms of the compatibility between the polymer matrix and MMT. In addition, the mechanical properties of PP/MMT nanocomposites were improved. A simultaneous increase in the tensile strength and toughness was observed in PP/PMOM nanocomposites.
 J. Appl. Polym. Sci. 128: 3876–3884, 2013

KEYWORDS: clay; compatibilization; rheology; polyolefins

Received 18 July 2012; accepted 19 September 2012; published online 12 October 2012
DOI: 10.1002/app.38626

INTRODUCTION

Since the first successful nylon/clay nanocomposites was invented by Toyota researchers in 1980 s, polymer/clay nanocomposites (PCN) have attracted substantial attention in the polymer industry as a new type of composite material because of their superior properties (including high heat deflection temperature, gas barrier performance, dimensional stability, enhanced mechanical properties, optical clarity, and decreased flammability) when compared with the pure polymers or conventional composites.[1–3] Depending on the interfacial interactions between the polymer chains and clay layers, final structure of PCN could be exfoliated or intercalated.[4,5]

From the point of view of obtaining markedly improved mechanical properties of PCN, exfoliation is preferred to intercalation. In general, intercalation is observed when a polymer matrix and clay do not have sufficient attractive interactions, while exfoliation is observed when a polymer matrix and clay have strong attractive interactions.[5] Good compatibility between clay and polymer matrix is necessary to achieve a high degree of exfoliation of clay aggregates and thus improved mechanical properties of PCN. Thus, a fundamental issue in the preparation of PCN is how to provide strong attractive interactions between clay and polymer matrix.[6]

Polypropylene (PP) is one of the most widely used thermoplastics because of its attractive combination of good process ability and mechanical properties. However, its inadequate brittleness limits its versatile application to some extent. An effective and economical method to improve the mechanical properties of PP is compounding with montmorillonite (MMT).[7,8] Because the backbone of PP has no any polar groups, it is very difficult to directly prepare intercalation or exfoliation PP/MMT nanocomposites. Lots of efforts were made to improve the compatibility between MMT and PP matrix by using functional oligomers as compatibilizer.[9–16] The most widely used compatibilizer was maleic anhydride modified PP (PP-*g*-MA). The driving force of the intercalation originated from the hydrogen bonding between the COOH group generated from the hydrolysis of maleic group and the oxygen groups of silicates.[17,18] The effects of PP-*g*-MA

Table I. Chemical Structure of the Three Modifiers

	PEG	alkyl-PEG	PP-*g*-PEG
Structure	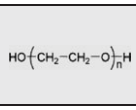	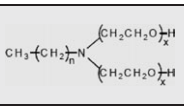	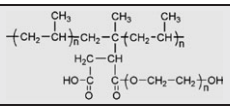

on composites morphology and the correlation between the achieved morphology and the material properties are widely investigated.[19–23] The results showed that MMT was not only well dispersed, but also exfoliated. The modulus and tensile strength and thermal properties of PP/MMT nanocomposites were enhanced while the melt viscosity and toughness were no obvious improvement.

Rheological studies of PCN have been of interest recently because such studies offer a way to characterize the state of dispersion of layer silicate, and also provide useful guidelines for optimum processing conditions. The significance of compatibilizer (PP-*g*-MA) on the rheological behavior of PP/MMT nanocomposites was studied by Galgali et al.[24] The zero shear viscosity (η_0) of compatibilized nanocomposites was three-orders of magnitude higher than that of the matrix and uncompatibilized nanocomposites, indicating that the presence of PP-*g*-MA enhanced the exfoliated structure. Gu et al.[25] showed that at lower frequencies, the steady shear viscosities of PP/MMT nanocomposites increased with the organo-montmorillonite (OMMT) content. However, the PP/MMT nanocomposites melts showed a greater shear-thinning tendency than pure PP melt because of the preferential orientation of the MMT layers. They concluded that the PP/MMT nanocomposites had higher moduli but better processability compared with pure PP. Using oscillatory shear experiments, Li et al.[26] reported that the percolation threshold for PP/MMT nanocomposites was observed with clay loadings near 3 wt %, while Salomon et al.[27] found a percolation threshold around 2 wt %.

The rheological behavior of PP/MMT nanocomposites depends on the degree of dispersion of MMT aggregates, which in turn depends, among many factors, on the degree of compatibility between polymer matrix and MMT.[28] Note that MMT has a large active surface area and a moderate negative surface charge. Upon replacing the hydrated metal cation from the interlayers of the pristine MMT with organic cations such as an alkyammonium, the MMT attains a hydrophobic/organophilic character, which typically results in large interlayer spacing.[1] Because the negative charge originates in the MMT, the cationic head groups of the alkylammonium chloride molecule preferentially reside at the surface of the MMT, while the oligomeric tallow species, which sometime contain polar groups, extend into the galleries. Therefore, it is very important to match the chemical affinity between a polymer matrix and MMT in order to achieve a very high degree of exfoliation of OMMT platelets in a polymer matrix.[3]

In this study, we have investigated the melt rheology of PP/MMT nanocomposites by using Ca^{2+}-MMT and OMMT treated with octadecyl trimethylammonium chloride. We chose three modifiers with decreasing polarity: poly(ethylene glycol) (PEG), octadecyl amine ethoxylate ether (alkyl-PEG) with two poly(ethylene oxide) chains, and PEG *grafted* PP (PP-*g*-PEG) (Table I). The rationale behind the choice of these modifiers was the following. PEG was easily intercalated into the galleries of MMT. And the interaction between PEG and MMT was rather strong.[29] We were able to control the degree of polarity by functional PEG. Thus, in this study we investigated the rheological behavior of PP/MMT nanocomposites having different compatibilities between MMT and polymer matrix. The PP/MMT nanocomposites were characterized using X-ray diffraction (XRD) and transmission electron microscopy (TEM) before rheological measurements were made. Then we investigated the linear dynamic viscoelasticity of the PP/MMT nanocomposites, with emphasis on the effects of polymer/matrix compatibility.

EXPERIMENTAL

Materials

A commercially available isotactic PP (F401) was supplied from Lanzhou Chemical Industry Factory (Lanzhou, China), with a melt flow index of 2.5 g/10 min (190°C, 2.16 kg). Ca^{2+}-MMT with a cation exchange capacity (CEC) of 90 mmol/100 g and OMMT was supplied by Zhejiang Fenghong Clay Chemicals Co. (Zhejiang, China). OMMT was sodium MMT modified with octadecyl trimethylammonium chloride. PEG was supplied by Liaoyang Aoke Chemical Co. (Liaoning, China) with a molecular weight of 6000. PP-*g*-PEG was prepared by the esterification between PP-*g*-MA and PEG according to the literature.[30] Octadecyl amine ethoxylate ether (alkyl-PEG) was purchased from Haian Petroleum Chemical Co. (Jiangshu, China), which was used as surfactant and the molecular structure ($n = 17$, $x = 30$) is shown in Table I.

Modification of Montmorillonite

PEG (50 g) was first dissolved in water till limpid solution was obtained and then Ca^{2+}-MMT (50 g) was added to this surfactant solution. The dispersion was heated at 60°C under vigorous stirring. The PEG/Ca^{2+}-MMT (PM) hybrids were dried in an oven at 60°C for several days and then pulverized. The power was sieved by passing through a 200-mesh stainless steel sifter. PEG/OMMT (POM), alkyl-PEG/Ca^{2+}-MMT (AM), alkyl-PEG/OMMT (AOM), PP-*g*-PEG/Ca^{2+}-MMT (PMM), and PP-*g*-PEG/OMMT (PMOM) hybrids were all prepared in the same way. Abbreviations of the modified MMT prepared with different modifiers are listed in Table II.

Table II. Abbreviation of the Modified MMT Prepared with Different Modifiers

Modifier	Montmorillonite	Weight ratio	Abbreviation
PEG	Ca^{2+}-MMT	1 : 1	PM
	OMMT	1 : 1	POM
alkyl-PEG	Ca^{2+}-MMT	1 : 1	AM
	OMMT	1 : 1	AOM
PP-*g*-PEG	Ca^{2+}-MMT	1 : 1	PMM
	OMMT	1 : 1	PMOM

Applied Polymer SCIENCE

Sample Preparation

These modified MMT were added with 1–5 parts per hundred parts of PP (phr) by weight, then extruded by a general three-section twin-screw extruder (D = 20 mm, L/D = 40). Screw speed was set at 200 rpm and the temperatures were 175°C, 190°C, and 190°C for each section of the barrel and 185°C for the die. An injection-molding machine (K-TEC400, Klarke international Co., Germany) was used to prepare the specimens for the mechanical tests.

Characterization

X-Ray Diffraction. XRD patterns were collected on X'Pert Pro X-ray diffractometer using Ni-filtered Cu KR radiation from 1.5° to 30°, the scanning speed being 2°/min with a step of 0.03°. Powder samples were packed in horizontally held trays. The changes in the XRD peak positions reflect the intercalation of the polymer into layered silicates. The Bragg equation was applied to calculate the basal spacing of MMT platelets. The gallery sizes in intercalated hybrids were deduced from XRD peak positions (001) of the hybrids.

Transmission Electron Microscopy. TEM was carried out with an H-7100 (Tokyo, Japan) instrument with an accelerating voltage of 100 kV. The ultra-thin sections of the samples from injection molded with a thickness of 50 nm were cut at 20°C by a Reichert Ultracut cryoultramicrotome without staining.

Rheological Measurements. Viscoelastic behaviors of the nanocomposites were analyzed by a Bohin Gemini 2000 rheometer (Malvern Instruments, England) in the melt state. The rheometer equipped with 25 mm diameter parallel plate geometry was employed for the rheological tests. Samples were directly loaded and molded between the plates and rheological tests were carried out at 190°C with a gap distance of 1 mm under nitrogen atmosphere. First, strain sweep test was performed from the initial strain value of 0.1 to a final strain value of 100 in percent, with the frequency of 1 s^{-1} to determine the linear viscolelastic region of the samples. Storage modulus (G') and loss modulus (G'') were recorded as a function of shear strain (γ %). G' and dynamic viscosity (η^*) were measured as a function of angular frequency (ω) in the range of 0.01–100 s^{-1} at a strain value in the linear viscoelastic region (strain magnitude of 0.02).

Mechanical Test. Tensile tests were carried out according to GB/T 1040-92 standard on CMT 4104 machine (Sans Material Testing Technical Co., Shenzhen, China). Elongation at break was measured at a cross-head speed of 50 mm/min. Izod-notched impact strength was measured with ZQK-20 (Dahua Material Testing Technical Co., China) according to GB/T1043-93 standard.

RESULTS AND DISCUSSION

Phase Morphology in PP/MMT Nanocomposites

Figure 1 shows the XRD patterns of Ca^{2+}-MMT, OMMT, and their composites. Notice in Figure 1(a) that Ca^{2+}-MMT has a gallery distance (d_{001} spacing) of 1.51 nm. The d_{001} spacing of PM increased to 1.77 nm. This increase can be attributed to the PEG chains intercalation between Ca^{2+}-MMT layers. However, the d_{001} spacing of Ca^{2+}-MMT in PP/PM composites was almost unchanged when compared with PM hybrids, indicating

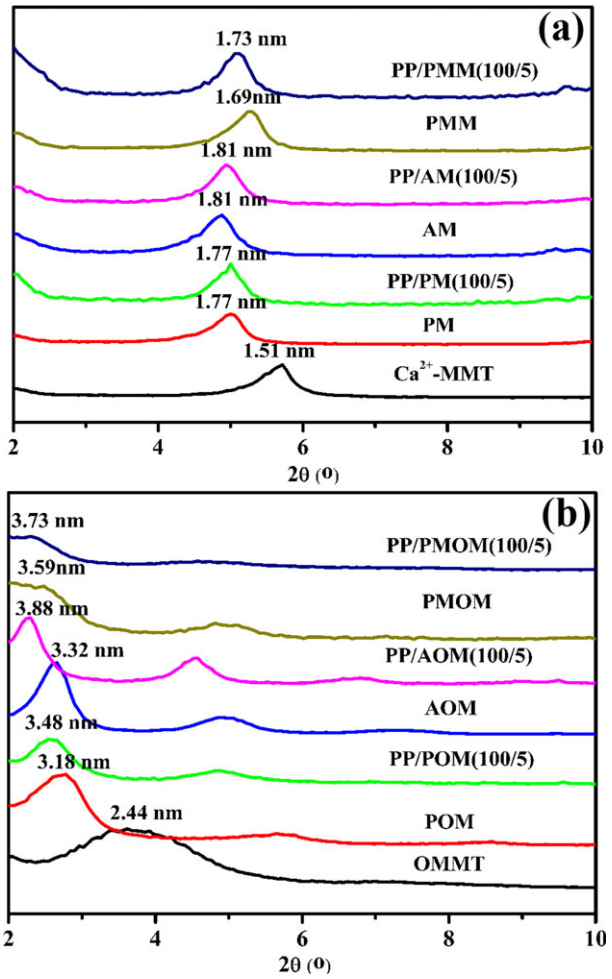

Figure 1. XRD patterns for MMT and PP/MMT composites: (a) Ca^{2+}-MMT systems, (b) OMMT systems. [Color figure can be viewed in the online issue, which is available at wileyonlinelibrary.com.]

that there were no PP chains that can diffuse into the interlayer space of PM hybrids in these composites. A similar result was observed in PP/AM composites. When PP was melt blend with PMM hybrids, the d_{001} spacing of PP/PMM composites increased a little. These results indicated that melt blending with PP did not lead to further intercalation of the modified Ca^{2+}-MMT and formed a micro-composites structure.

The d_{001} spacing of OMMT was 2.44 nm [Figure 1(b)]. The d_{001} spacing of POM increased to 3.18 nm. The basal spacing of OMMT in PP/POM was larger than that of POM. The same results were found in PP/AOM and PP/PMOM composites. These increases could be attributed to the intercalated PEG chains and PP chains in the interlayer space of OMMT. These results indicated that modified OMMT melt blending with PP had led to further intercalation and formed a nanostructure. The PP/POM nanocomposite had a d_{001} spacing of 3.48 nm, while the PP/AOM nanocomposite had a d_{001} spacing of 3.88 nm, an increase of 1.44 nm over the d_{001} spacing of OMMT. This result suggested that the degree of intercalation of AOM in PP was higher than that of POM. PP/PMOM nanocomposite exhibited a weak intensity and broad peak, suggesting that

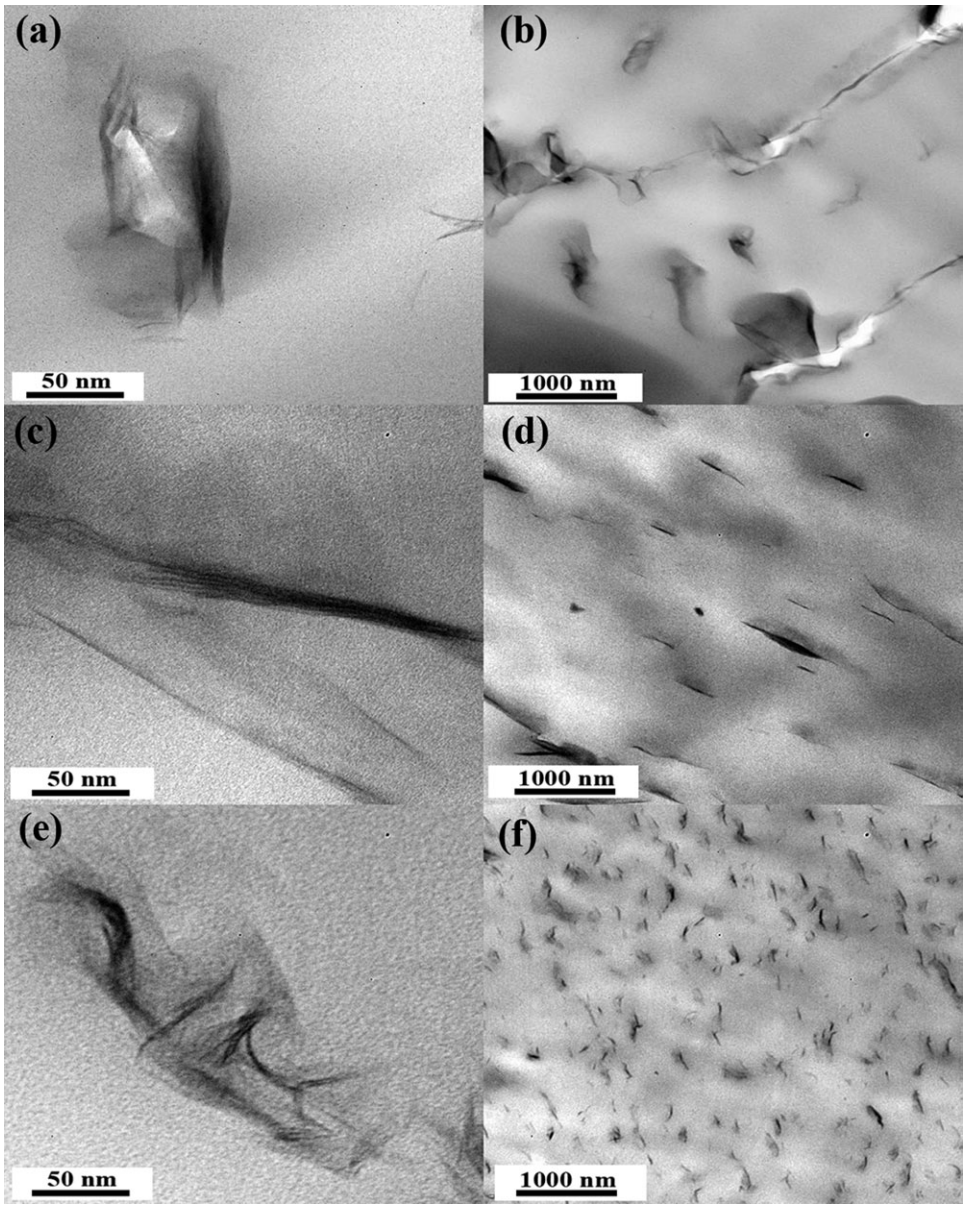

Figure 2. TEM micrographs of PP/OMMT nanocomposites: (a,b), PP/POM (100/5); (c,d), PP/AOM (90/10/5); (e,f), PP/PMOM (100/5).

PMOM might have been reasonably well dispersed (exfoliated to a certain degree) in PP matrix. The differences in XRD patterns among the three PP/MMT nanocomposites seemed to indicate that PP-*g*-PEG was the most effective in dispersing OMMT in PP matrix, while the alkyl-PEG was better than PEG. Although XRD patterns may not be regarded as being the most sensitive measure for describing the degree of intercalation or exfoliation of OMMT in a polymer matrix, they certainly were very useful to make qualitative observations.

To further confirm the microstructure, the TEM of PP/POM (100/5), PP/AOM (100/5), and PP/PMOM (100/5) nanocomposites were performed. Bright field was the image of polymer matrix, in which dark entities represented the cross-section of intercalated silicate layers. The following observations were worth noting in Figure 2. Within experimental uncertainties, the degree of intercalation of AOM in the PP/AOM nanocomposite was higher than that of POM in the PP/POM nanocomposite. This observation was consistent with that made from the XRD patterns given in Figure 1(b). Notice in Figure 2(b) that the very large POM aggregates were not even well dispersed in the PP/POM nanocomposite, suggesting that POM and PP had very poor compatibility. The degree of dispersion of PMOM aggregates in the PP/PMOM nanocomposite [Figure 2(f)] was considerably higher than that in the PP/AOM nanocomposite [Figure 2(d)]. A reasonably high degree of dispersion of PMOM in the PP matrix was attributed to the existence of attractive interactions, via hydrogen bonding, between the COOH group generated from maleic group and the polar MMT surface.[15,17,18] The above observation was consistent with that made from the XRD patterns given in Figure 1.

Applied Polymer SCIENCE

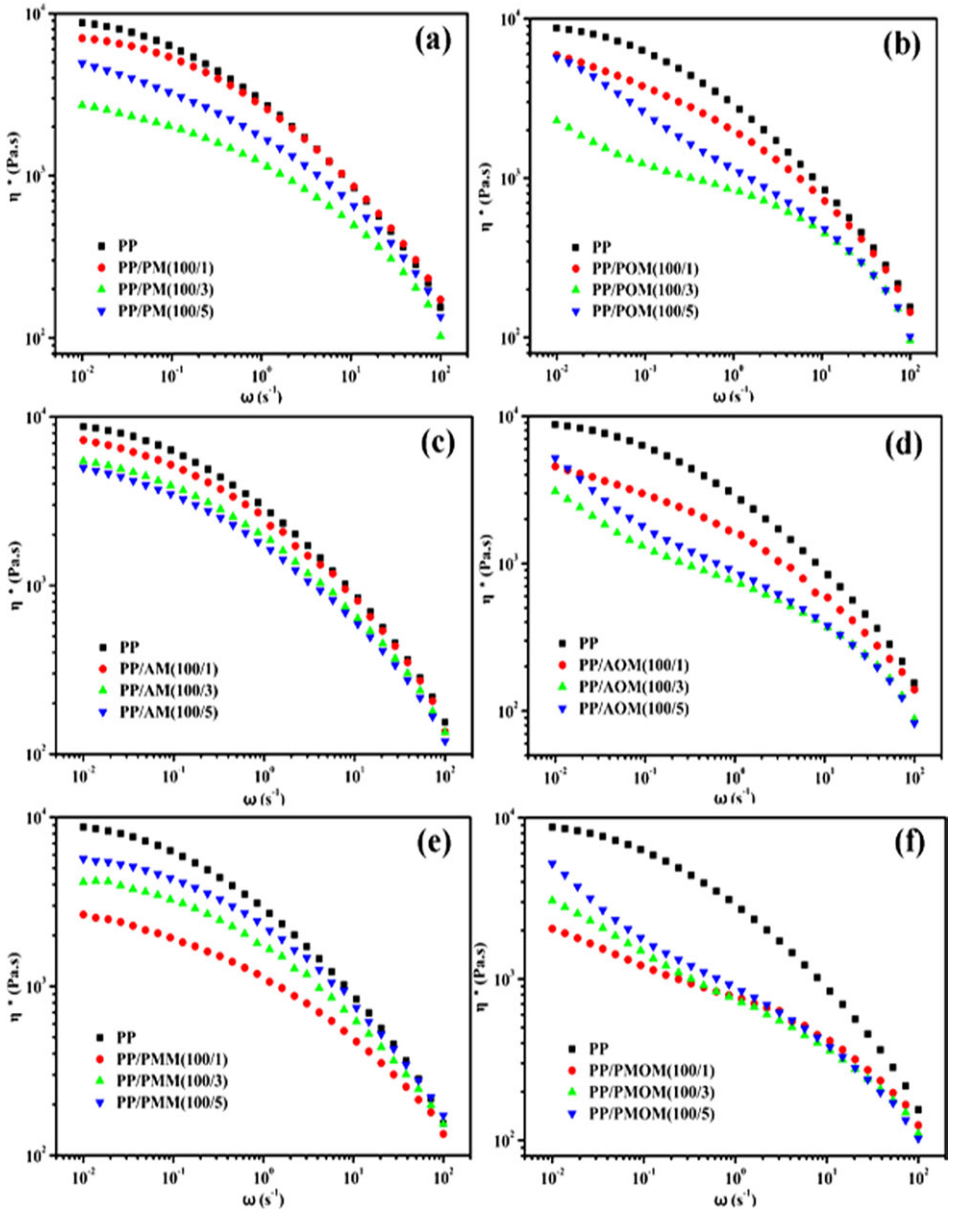

Figure 3. Complex viscosities from oscillatory tests in the linear viscoelastic region on PP/MMT nanocomposite melts at 190°C. [Color figure can be viewed in the online issue, which is available at wileyonlinelibrary.com.]

Linear Viscoelasticity of PP Nanocomposites

Small amplitude dynamic rheology measurements were used to evaluate the linear viscoelasticity of PP nanocomposites in the shear state. Figure 3 shows log η^* as a function of log ω for neat PP and PP nanocomposites, in which values of complex viscosity η^* were calculated using the followed relationship:

$$|\eta^*| = \sqrt{(G'/\omega)^2 + (G''/\omega)^2} \quad (1)$$

Neat PP exhibited the typical behavior for a polymer, including a tendency to the low shear Newtonian plateau and a shear thinning region. Upon adding the modified MMT, the shear viscosities of all PP/MMT composites decreased. This rheological behavior was different from most surfactant modified PP/MMT nanocomposites which typically showed an increase in dynamic modulus and viscosity relative to the PP matrix.[24] There were two factors affecting the viscoelastic behaviors of PP/MMT nanocomposites. On the one hand, the reduction of complex viscosity relative to the PP matrix can be attributed to the plasticization effect of PEG segments in the three modifiers. The mobility of PP chains increased due to PEG behavior as plasticizer. On the other hand, PP chains limited by the fact that adding MMT would increase the viscosity of PP/MMT nanocomposites. In Figure 3(a,b), PP shows a clear increase in η^* when added 5 phr PM and POM. It was because the plasticization effect of PEG segments was gradually balanced by the increased PM and POM. The complex viscosity of PP/AM

composites decreased with the AM loading [Figure .3(c)]. PP/AOM nanocomposite showed a clear increase in η^* when the AOM content was 5 phr. However, the complex viscosities of PP/PMM and PP/PMOM nanocomposites increased with the MMT loading. PP/PMOM nanocomposites always exhibited a yield stress with increasing the PMOM loading at low frequency ($< 1\ s^{-1}$). It suggested that the surface of, at least, the well-dispersed PMOM was sufficiently compatible with PP to enable dispersion of the layer silicates in the PP matrix and formation of a network structure. These rheological behaviors were attributed to the strong interaction between PP and PMOM when compared with PP/POM and PP/AOM nanocomposites.

In order to detected the effect of compatibility on rheological behaviors of PP/MMT nanocomposites. The flow curves taken under small amplitude measurement conditions were fitted to the power law expression:

$$\eta = k\omega^n \tag{2}$$

where η is dynamic viscosity; k is a sample specific factor; ω is the oscillation frequency of the rheometer equivalent to shear rate; and n is the shear thinning exponent.[31,32] In order to determine k and n, a plot of log (η) vs. log (ω) was made and fitted to a straight line.

$$\mathrm{Log}(\eta) = \mathrm{Log}k + n\mathrm{Log}(\omega) \tag{3}$$

The shear thinning exponent n is the proposed semi-quantitative measure of the MMT dispersion in PP matrix.[33,34] In this study, power law model was applied to complex viscosity (η^*) curves of the samples in low frequency region (between the frequency of 0.1 and 0.01 s^{-1}). We can compare the n values for the different PP/MMT nanocomposites prepared at the same composition and processing conditions in order to understand how melt rheology differs depending on the compatibilities between modified OMMT and PP matrix.

Figure 4 shows the results obtained with PP and three different PP/MMT nanocomposite samples. The neat PP exhibited the typical Newtonian behavior at the comparatively low shear rates employed here, resulting in a shear thinning exponent $n = -0.08$. The three PP/MMT nanocomposites comprising PEG modified OMMT platelets did show pronounced shear thinning. The exponent n values of PP/POM, PP/AOM, and PP/PMOM nanocomposites were -0.34, -0.40, and -0.51, respectively. Clearly, the shear thinning exponent allowed a quantitative discrimination on the compatibilities between MMT and PP matrix. The stronger the interactions between the MMT and the PP matrix, the higher the absolute value of shear thinning exponent. High absolute value of shear thinning exponent n indicated well dispersed OMMT layers in the PP matrix. Thus, the compatibilities of the three modifiers increases from PEG to alkyl-PEG and then to PP-*g*-PEG.

Figure 5 shows the dependence of storage modulus (G') on frequency (ω) for the PP nanocomposite series of different modified OMMT with various loadings. It was clearly seen that OMMT addition influences the storage modulus and this effect was especially more pronounced at low frequencies. As the

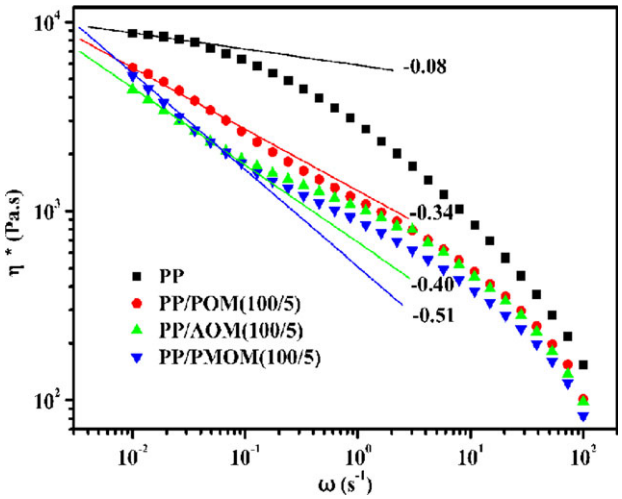

Figure 4. Flow curves log (η) vs. log (ω) of different PP/MMT nanocomposite samples prepared by melt blending under identical processing conditions. [Color figure can be viewed in the online issue, which is available at wileyonlinelibrary.com.]

OMMT amount increases, the G' increased and the slope of the G' decreased at low frequency region. A plateau in the storage modulus was indicative of the formation of a percolated network, leading to slow solid-like relaxation. Low frequency plateaus in G' had been interpreted as arising from the dispersion of the OMMT to form a house-of-cards network structure in the polymer matrix.[35,36] The plateau values of G' observed for PP/POM(100/5), PP/AOM(100/5), and PP/PMOM(100/5) nanocomposites were about 60, 80, and 95 Pa, respectively. The magnitude of the G' plateau was on the order of k_BT/d^3 (where k_BT is the Boltzmann constant times the absolute temperature and d is the characteristic length scale of the MMT network). This relation can be used to estimate the characteristic length scale.[37] The OMMT network of PP/POM (100/5), PP/AOM (100/5), and PP/PMOM (100/5) nanocomposites were percolated as $d \approx 41$, 37, and 35 nm, respectively. It indicated that the characteristic length scale was relative to the compatibilities between the OMMT and the PP matrix. The stronger the interactions between the OMMT and the PP matrix, the lower the characteristic length scale. Low value of characteristic length scale indicated better dispersed OMMT layers in the PP matrix.

As discussed in Figure 3, the addition of the modified OMMT to the PP led to a small (≈10–20%) decrease in the moduli, G' and G'' (and therefore in the complex viscosity, η^*). Thus, the addition of the modified OMMT appeared to plasticize the PP matrix and decreased the complex viscosity. This rheological behavior was unusual because polymer nanocomposites based on surfactant modified MMT typically showed an increase in viscosity relative to the matrix polymer.[25,27,28,32] The three types of modified OMMT influenced the rheology both at low frequencies (where the well-dispersed fraction of the OMMT formed an elastic network, indicating compatibility with the PP) and at high frequencies (where the matrix PP was plasticized). This combination of an enhanced low frequency modulus and plasticization at high frequencies led to an enhanced

Applied Polymer SCIENCE

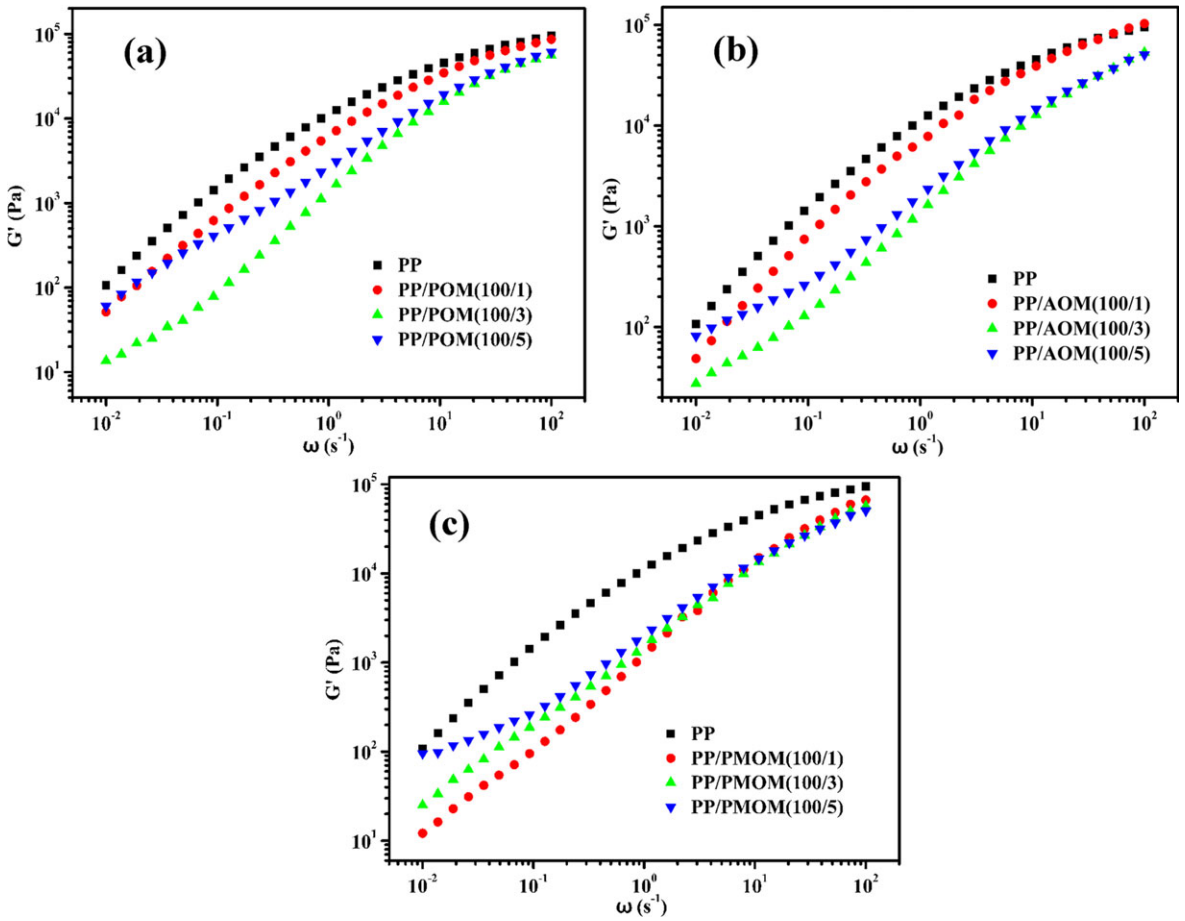

Figure 5. Storage modulus (G') of the PP nanocomposites prepared with different modified OMMT. [Color figure can be viewed in the online issue, which is available at wileyonlinelibrary.com.]

apparent shear thinning that might be advantageous for processing.

Mechanical Properties of PP and PP Nanocomposites

The mechanical properties of the pure PP and the PP/MMT composites are illustrated in Table III. With the addition of Ca-MMT, all mechanical properties of PP decreased. But in PP/OMMT composites, these properties increased marginally. The PP/PM and PP/POM composites showed a little decrease in tensile strength relative to neat PP. A similar result was observed in the PP/AM and PP/AOM nanocomposites. However, their Izod-notched impact strength and elongation at break increased. This could be attributed to the plasticization of modifier with PEG segments. The tensile strength of PP/PMM and PP/PMOM nanocomposites increased. This agreed well with our melt rheological data that suggested that the MMT modified by PP-*g*-PEG was more effectively dispersed in PP matrix than POM and AOM. For conventional polymer-clay nanocomposites, the

Table III. The Mechanical Properties of PP and PP/MMT(100/5) Composites

Sample	Tensile strength (MPa)	Elongation at break (%)	Impact strength (kJ/m^2)
PP	31.0 ± 0.5	83.9 ± 5.8	4.0 ± 0.3
PP/Ca-MMT	30.2 ± 0.3	66.3 ± 4.1	3.8 ± 0.2
PP/OMMT	31.6 ± 0.4	105.1 ± 6.6	4.4 ± 0.3
PP/PM	30.6 ± 0.2	81.3 ± 4.3	7.0 ± 0.4
PP/POM	30.5 ± 0.5	205.8 ± 11.2	11.8 ± 0.6
PP/AM	28.7 ± 0.3	125.7 ± 4.3	6.0 ± 0.3
PP/AOM	29.4 ± 0.6	254.2 ± 12.0	11.1 ± 0.4
PP/PMM	33.2 ± 0.5	125.7 ± 3.2	6.0 ± 0.4
PP/PMOM	32.5 ± 0.8	117.3 ± 5.1	7.3 ± 0.2

increase in modulus typically came at the expense of decreased toughness (viz. decreased impact strength) and decreased ductility.[2,38–40] However, PP/PMOM nanocomposites showed a marginal increase in elongation at break and impact strength relative to the PP. For example, When 5 phr of PMOM was added, the Izod-notched impact strength and elongation at break of PP increased by 82.5% and 39.8%, respectively. A simultaneous increase in the tensile strength, and in the ductility and toughness, was unusual and was certainly not anticipated for polymer clay micro- or nanocomposites. The relative flexibility of the interface between PP and PMOM might lead to the observed balance of mechanical properties. When the PMOM dispersed in the PP, the layers formed networks that resulted in a higher tensile strength; however, the failure properties were not adversely affected probably due to the redundant PP-*g*-PEG which had a little plasticization effect in PP matrix. Because of the lower effective PEG content of PP-*g*-PEG, the plasticization effect of PMOM was less than POM and AOM. Hence, the improvements in impact strength and elongation at break of PP/PMOM composites were not as good as PP/POM and PP/AOM composites. The weaker plasticization effect can also make the PP/PMOM composites stronger.

CONCLUSIONS

In this study, three modifiers with different compatibilities (PEG, alkyl-PEG, and PP-*g*-PEG) were chosen to modify Ca^{2+}-MMT and OMMT. The PP/MMT nanocomposites were characterized using XRD and TEM before rheological measurements were made. XRD results indicated that all the three modifiers can intercalate into the interlayer space of Ca^{2+}-MMT and OMMT. PP chains can diffuse into the interlayer space of modified OMMT but not into Ca^{2+}-MMT. TEM showed the degree of dispersion of OMMT in the PP/PMOM nanocomposite was considerably higher than those in the PP/POM and PP/AOM nanocomposites. It indicated that the dispersion was relative to the compatibility between modified OMMT and PP matrix. Linear viscoelasticity of PP nanocomposites in shear flow was investigated by low amplitude dynamic measurements. Upon adding the modified MMT, the shear viscosities and storage modulus of all PP/MMT composites decreased. This rheological behavior was different from most surfactant modified PP/MMT nanocomposites which typically showed an increase in dynamic modulus and viscosity relative to the polymer matrix. In addition, the mechanical properties of PP/MMT composites were improved. A simultaneous increase in the tensile strength and toughness was observed in PP/PMOM nanocomposites.

ACKNOWLEDGMENTS

This work was supported by the Program for New Century Excellent Talents in University (NCET-10-0562) and the National Basic Research Program of China (2005CB623800).

REFERENCES

1. Sinha Ray, S.; Okamoto, M. *Prog. Polym. Sci.* **2003**, *28*, 1539.
2. Okada, A.; Usuki, A. *Macromol. Mater. Eng.* **2006**, *291*, 1449.
3. Pavlidou, S.; Papaspyrides, C. *Prog. Polym. Sci.* **2008**, *33*, 1119.
4. Xie, X. L.; Mai, Y. W.; Zhou, X. P. *Mater. Sci. Eng., R* **2005**, *49*, 89.
5. Liu, J.; Boo, W. J.; Clearfield, A.; Sue, H. *J. Mater. Manuf. Processes* **2006**, *21*, 143.
6. Tjong, S. *Mater. Sci. Eng. R* **2006**, *53*, 73.
7. Zhu, S.; Chen, J.; Li, H. *Polym. Bull.* **2009**, *63*, 245.
8. Zhu, S.; Chen, J.; Zuo, Y.; Li, H.; Cao, Y. *Appl. Clay. Sci.* **2011**, *52*, 171.
9. Cui, L. L.; Paul, D. R. *Polymer* **2007**, *48*, 1632.
10. Szazdi, L.; Pukanszky, B.; Foldes, E.; Pukanszky, B. *Polymer* **2005**, *46*, 8001.
11. Lopez-Quintanilla, M. L.; Sanchez-Valdes, S.; de Valle, L. F. R.; Miranda, R. G. *Polym. Bull.* **2006**, *57*, 385.
12. Chen, H. W.; Chang, F. C. *Polymer* **2001**, *42*, 9763.
13. Wang, Z. M.; Han, H.; Chung, T. C. *Macromol. Symp.* **2005**, *225*, 113.
14. Garcia-Lopez, D.; Picazo, O.; Merino, J. C.; Pastor, J. M. *Eur. Polym. J.* **2003**, *39*, 945.
15. Kawasumi, M.; Hasegawa, N.; Kato, M.; Usuki, A.; Okada, A. *Macromolecules* **1997**, *30*, 6333.
16. Moncada, E.; Quijada, R.; Lieberwirth, I.; Yazdani-Pedram, M. *Macromol. Chem. Phys.* **2006**, *207*, 1376.
17. Hasegawa, N.; Kawasumi, M.; Kato, M.; Usuki, A.; Okada, A. *J. Appl. Polym. Sci.* **1998**, *67*, 87.
18. Hasegawa, N.; Okamoto, H.; Kato, M.; Usuki, A. *J. Appl. Polym. Sci.* **2000**, 78, 1918.
19. Joshi, M.; Viswanathan, V. *J. Appl. Polym. Sci.* **2006**, *102*, 2164.
20. Kodgire, P.; Kalgaonkar, R.; Hambir, S.; Bulakh, N.; Jog, J. P. *J. Appl. Polym. Sci.* **2001**, *81*, 1786.
21. Kanny, K.; Jawahar, P.; Moodley, V. K. *J. Mater. Sci.* **2008**, *43*, 7230.
22. Chiu, F. C.; Lai, S. M.; Chen, J. W.; Chu, P. H. *J. Polym. Sci. Part B: Polym. Phys.* **2004**, *42*, 4139.
23. Mittal, V. J. *Thermoplast Compos.* **2007**, *20*, 575.
24. Galgali, G.; Ramesh, C.; Lele, A. *Macromolecules* **2001**, *34*, 852.
25. Gu, S. Y.; Ren, J.; Wang, Q. F. *J. Appl. Polym. Sci.* **2004**, *91*, 2427.
26. Li, J.; Zhou, C.; Wang, G.; Zhao, D. *J. Appl. Polym. Sci.* **2003**, *89*, 3609.
27. Solomon, M. J.; Almusallam, A. S.; Seefeldt, K. F.; Somwangthanaroj, A.; Varadan, P. *Macromolecules* **2001**, 34, 1864.
28. Wang, Y.; Chen, F. B.; Wu, K. C.; Wang, J. C. *Polym. Eng. Sci.* **2006**, *46*, 289.
29. Aranda, P.; Ruiz-Hitzky, E. *Appl. Clay Sci.* **1999**, *15*, 119.
30. Tang, T.; Lia, L. X.; Huang, B. T. *Eur. Polym. J.* **1994**, *30*, 5.

31. Samyn, F.; Bourbigot, S.; Jama, C.; Bellayer, S.; Nazare, S.; Hull, R.; Fina, A.; Castrovinci, A.; Camino, G. *Eur. Polym. J.* **2008**, *44*, 1631.

32. Zhao, J.; Morgan, A. B.; Harris, J. D. *Polymer* **2005**, *46*, 8641.

33. Durmus, A.; Kasgoz, A.; Macosko, C. W. *Polymer* **2007**, *48*, 4492.

34. Samyn, F.; Bourbigot, S.; Jama, C.; Bellayer, S.; Nazare, S.; Hull, R.; Castrovinci, A.; Fina, A.; Camino, G. *Eur. Polym. J.* **2008**, *44*, 1642.

35. Abranyi, A.; Szazdi, L.; Pukanszky, B., Jr.; Vancso, G. J.; Pukanszky, B. *Macromol. Rapid Commun.* **2006**, *27*, 132.

36. Okamoto, M.; Nam, P. H.; Maiti, P.; Kotaka, T.; Hasegawa, N.; Usuki, A. *Nano Lett.* **2001**, *1*, 295.

37. Kumaraswamy, G.; Deshmukh, Y. S.; Agrawal, V. V.; Nisal, A. A. *Ind. Eng. Chem. Res.* **2008**, *47*, 3891.

38. Luo, J. J.; Daniel, I. M. *Compos. Sci. Technol.* **2003**, *63*, 1607.

39. Deshmane, C.; Yuan, Q.; Perkins, R.; Misra, R. *Mater. Sci. Eng. A* **2007**, *458*, 150.

40. Ganguli, S.; Dean, D.; Jordan, K.; Price, G.; Vaia, R. *Polymer* **2003**, *44*, 1315.